



Universidad Autónoma
de Madrid

Biblos-e Archivo
Repositorio Institucional UAM

Repositorio Institucional de la Universidad Autónoma de Madrid

<https://repositorio.uam.es>

Esta es la **versión de autor** del artículo publicado en:

This is an **author produced version** of a paper published in:

Science of the Total Environment 761 (2021): 143213

DOI: <https://doi.org/10.1016/j.scitotenv.2020.143213>

Copyright: © 2020 Elsevier B.V. This manuscript version is made available under the CC-BY-NC-ND 4.0 licence <http://creativecommons.org/licenses/by-nc-nd/4.0/>

El acceso a la versión del editor puede requerir la suscripción del recurso

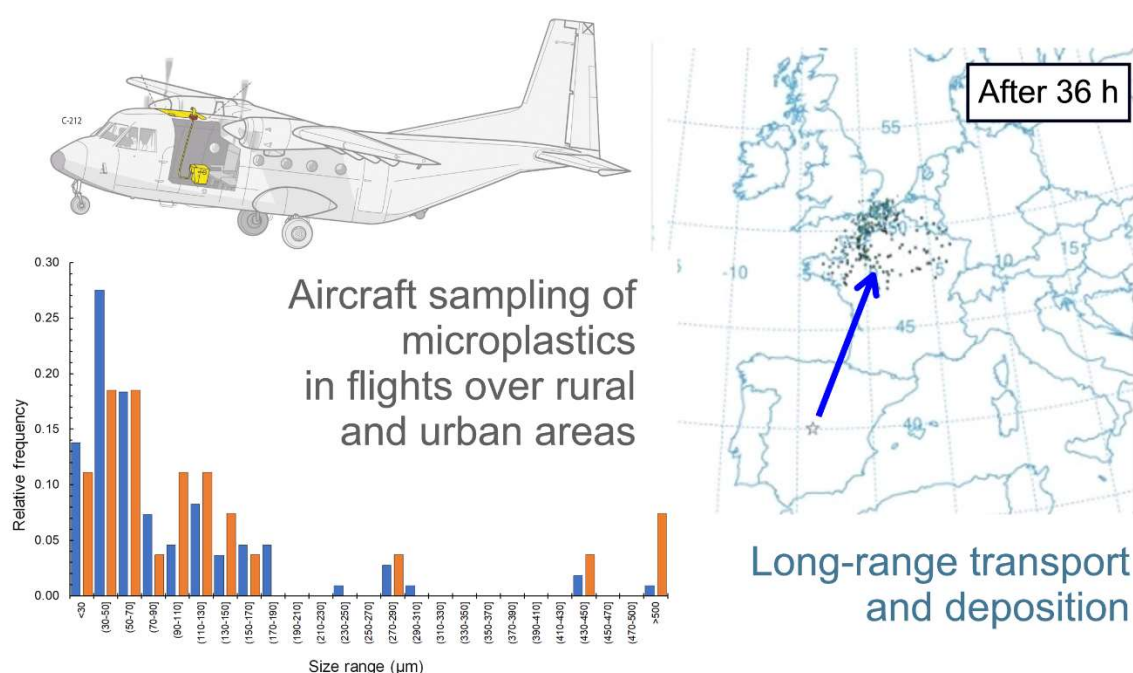
Access to the published version may require subscription

Occurrence and transport of microplastics sampled within and above the planetary boundary layer

This version is made available in accordance with publisher policies.

Please, cite as follows:

Miguel González-Pleiter, Carlos Edo, Ángeles Aguilera, Daniel Viúdez-Moreiras, Gerardo Pulido-Reyes, Elena González, Susana Osuna, Graciela de Diego, Francisco Leganés, Francisca Fernández-Piñas, Roberto Rosal, Occurrence and transport of microplastics sampled within and above the planetary boundary layer, *Science of The Total Environment*, 143213, <https://doi.org/10.1016/j.scitotenv.2020.143213>.



Link to official URL: <http://www.sciencedirect.com/science/article/pii/S0048969720367449>

DOI: 10.1016/j.scitotenv.2020.143213

Occurrence and transport of microplastics sampled within and above the planetary boundary layer

Miguel González-Pleiter^{1,2, †,*}, Carlos Edo^{2, †}, Ángeles Aguilera³, Daniel Viúdez-Moreiras³, Gerardo Pulido-Reyes^{1,4}, Elena González³, Susana Osuna³, Graciela de Diego³, Francisco Leganés¹, Francisca Fernández-Piñas¹, Roberto Rosal²

- 1 Departamento de Biología, Facultad de Ciencias, Universidad Autónoma de Madrid, Cantoblanco, E-28049 Madrid, Spain.
- 2 Departamento de Ingeniería Química, Universidad de Alcalá, Alcalá de Henares, E-28871 Madrid, Spain.
- 3 Centro de Astrobiología, CAB (INTA-CSIC), Torrejón de Ardoz, Spain.
- 4 Eawag, Swiss Federal Institute of Aquatic Science and Technology, Ueberlandstrasse 133, 8600 Dübendorf, Switzerland

* Corresponding author: mig.gonzalez@uah.es

Abstract

Nowadays, there is no direct evidence about the presence of microplastics (MPs) in the atmosphere above ground level. Here, we investigated the occurrence, chemical composition, shape, and size of MPs in aircraft sampling campaigns flying within and above the planetary boundary layer (PBL). The results showed that MPs were present with concentrations ranging from 1.5 MPs m⁻³ above rural areas to 13.9 MPs m⁻³ above urban areas. MPs represented up to almost one third of the total amount of microparticles collected. Fourier Transform Infrared Spectroscopy allowed identifying seven types of MPs with the highest diversity corresponding to urban areas. Atmospheric transport and deposition simulations were performed using the HYbrid Single-Particle Lagrangian Integrated Trajectory (HYSPLIT) model. Air mass trajectory analyses showed that MPs could be transported more than one thousand kilometres before being deposited. This pioneer study is the first evidence of the microplastic presence above PBL and their potential long-range transport from their point of release even crossing distant borders.

Keywords: Airborne microplastics; Aircraft sampling; Atmospheric transport; Microplastics deposition; Planetary boundary layer

1. Introduction

The uncontrolled release of plastics to the environment is a cause for global concern. Plastic pollution is an obvious consequence of the improper management of plastic wastes, but it is also produced by the incidental abrasion and wearing of different goods (Bomgardner, 2017; Karbalaee et al., 2018; Knight et al., 2020). As a legacy from the marine origin of this research field, the term microplastic (MPs) refers to microparticles made of a polymeric matrix with their largest dimension ranging from 1 µm to 5 mm (Frias and Nash, 2019; GESAMP, 2019). MPs can easily move among ecosystems and cause hazardous effects to many organisms including humans due to their small size and persistence (Sharma and Chatterjee, 2017). The harmful effect

of MPs strongly depends on their size. While larger particles may cause physical impacts like internal abrasions and blockages, smaller particles may translocate to internal tissues potentially accumulating in the food webs (Chang et al., 2020; Wang et al., 2021). Besides, chemical associated to plastics, like additives included during manufacture, non-intentionally added substances, or pollutants retained from the environment, are an additional cause for concern due to the possible damage to the environment or human health (Fred-Ahmadu et al., 2020).

The fate of MPs depends on the interconnection of the environmental compartments. From all the environmental compartments, the atmosphere is the least studied regarding the occurrence and spatial distribution of MPs. It has been suggested

that atmospheric transport may play a significant role in the spreading of plastic pollution worldwide (Allen et al., 2019; Ganguly and Ariya, 2019; Zhang et al., 2019). Specifically, atmospheric transport would be responsible for the findings of MPs in areas far away from the main sources of pollution (Bergmann et al., 2019; Free et al., 2014; González-Pleiter et al., 2020b). Until now, the presence of MPs in the atmosphere has only been demonstrated through indirect deposition studies or sampling at ground or near to ground level (Dris et al., 2016; Klein and Fischer, 2019; Stanton et al., 2019). The highest concentrations have been reported in urban areas with concentrations generally in the order of a few MPs m⁻³ (Abbasi et al., 2019; Cai et al., 2017; Dris et al., 2017; Dris et al., 2015; Dris et al., 2016; Kaya et al., 2018; Klein and Fischer, 2019; Liu et al., 2019a; Liu et al., 2019c; Zhou et al., 2017). The size of airborne MPs varies from a few microns to the millimetre range with median values in the hundreds of microns range. Micro-Raman (μ Raman) and micro-Fourier Transform Infrared Spectroscopy (μ FTIR) have been used to identify the atmospheric MPs with the finding of more than a dozen different polymers (Cai et al., 2017; Dris et al., 2016; Liu et al., 2019b). Airborne anthropogenic material not also includes MPs, but other artificial substances like extruded cellulose and many natural microparticles that underwent industrial processing such as industrially processed cotton or wool and that may result in similar environmental concerns (Stanton et al., 2019).

The sources and fate of atmospheric MPs remain poorly understood. Despite their many potential origins, no clear evidence has been reported to date. As a new area of atmospheric science, the available data are still limited in the field. Specifically, the way MPs become dispersed and transported into the atmosphere and the factors influencing their deposition have not been fully clarified yet. It has been suggested that films and fragments are probably derived from the disintegration of larger plastic goods like plastic bags and packaging materials, among other probable origins like building materials, industrial emissions, agriculture and particles released from waste incineration and emissions from the wear and tear of car tires (Kole et al., 2017; Liu et al., 2019b; Wright et al., 2020). Airborne MPs are usually dominated by fibres that can be attributed to the wearing of textiles, either natural or man-made. Finally, it should be noted that little is

known about the movement of MPs in the atmosphere and the extent to which MPs can be transported with atmospheric air masses. The data available on air mass trajectory analysis combined with atmospheric deposition studies, suggest that the fate and dispersion of airborne MPs strongly depend on atmospheric conditions such as wind speed and direction, the occurrence of precipitations and particle size (Chen et al., 2019; Enyoh et al., 2019; Gasperi et al., 2018).

So far, the occurrence of MPs in the atmosphere has been studied at ground level or a few meters above ground level. Our hypothesis is that MPs are present at high altitude, even above the Planetary Boundary Layer (PBL). MPs are released mainly from urban areas, where they reach higher concentration, get to the atmosphere and are eventually transported by winds long distances before being deposited. Here, we investigated the occurrence, spatial distribution, shape, and chemical composition of MPs directly sampled in aircrafts flying up to ~3500 m above the sea level (a.s.l.) or ~2800 m above ground level (a.g.l.) over a high-density urban area (Madrid, Spain), a low-density urban area (Guadalajara, Spain), and rural and sub-rural areas in Central Spain. Furthermore, simulations were performed using the HYbrid Single-Particle Lagrangian Integrated Trajectory (HYSPLIT) model in order to evaluate the atmospheric transport and deposition of MPs. This study provided the first direct evidence of the occurrence of MPs at high altitude in the atmosphere and showed that the atmosphere is an important compartment for the environmental distribution of MPs.

2. Materials and Methods

2.1. Sample collection

Samples were obtained during three different flights of a CASA C-212 turboprop-powered cargo aircraft from the Spanish National Institute of Aerospace Technology in according to previous work. Incoming air was filtered using 25- μ m size opening stainless steel meshes fitted into Whatman filter holders, which were directly connected to air intake openings as shown in Fig. 1. Air sampling lines were located at the leading edge of the airplane (Fig. 1A) and into the air intake on both sides (Fig. 1B) of the engines in a way that potential collection of debris produced by the engines, propeller, spinner and aircraft fairing was avoided. This procedure allowed collecting

microparticles with an equivalent diameter down to 9.8 μm . Microparticles consisted of natural and artificial materials as well as synthetic polymers or MPs. Fig. S1 (Supplementary Material, SM) includes additional explanation on the nomenclature used in this work. Total airflow through the filters was measured using flowmeter 393 Series Float Style Rotameter (SKC, USA). Air output was measured from the filter directly using the flowmeter between three to six times during sampling. The pressure drop between both parts of the filters was calculated using the conditions of the air outside the aircraft and yielded values in the 3.1–3.7 kPa range. This means that a certain mass of almost stagnant air existed inside the filtration line and, therefore, turbulence should not affect the filtration procedure.

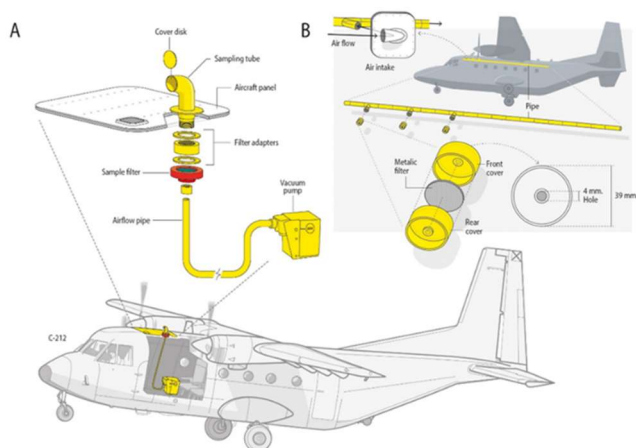


Figure 1. Aircraft scheme showing the location of air sampling lines. A: stainless steel filter holder inserted into the air intake, which opens at the leading edge of the airplane. B: filter holders inserted into the air intake on both sides of the aircraft.

2.2. Study area

The sampling campaigns consisted of three daytime flights that took place in the morning, approximately from 9 AM to 1 PM. Aircraft trajectories and sampling points were recorded for each flight and are shown in Fig. S2 (SM). In all flights, the aircraft took off from Torrejón Military Base. Flight 1 essentially flew all the time over rural areas. Flight 2 collected samples over the cities of Alcalá de Henares and Guadalajara and from Guadalajara to Valladolid flying over both rural and sub-urban areas. Flight 3 flew over Central Madrid (a high population density area: 5266 inhabitants km^{-2}) and Guadalajara (low-density area: 357 inhabitants km^{-2}). It is important

to note that the flight over Central Madrid was particularly complex due its highly restricted airspace. The total volume of air filtered was 8780 L taken between 701 m a.s.l. (the minimum altitude recorded on a flight) and 3496 m a.s.l. (the maximum altitude recorded on a flight; see additional details in Table S1, Supplementary Materials). In general, the average altitude of the flights was above planetary boundary layer (PBL), which ranges from 1.7 ± 0.5 km a.s.l. for the south of Spain (Granados-Muñoz et al. 2012) and between 0.5 and 1.5 km a.s.l. for the north of Spain (Banks et al. 2015). Thus, it can be considered that most of the microparticles were sampled above the PBL.

2.3. Quantification and identification of microparticles

Microparticles were defined as particles smaller than five mm along their largest dimension. Collected microparticles were measured and classified into fibres (microparticles with length/width ratio > 4) or fragments (microparticles with length/width ratio < 4) using a stereomicroscope Euromex-Edublu equipped with USB digital camera and ImageFocus 4 software. To avoid contamination, image acquisition was directly performed on the 25- μm stainless steel filters placed into their closed Petri dishes. A randomly distributed subsample of microparticles that included fibres and fragments of each filter in each area was selected for chemical identification (details are given in Table S1, SM). In total, one third of all the microparticles collected were analysed by μFTIR using a Perkin-Elmer Spotlight 200 Spectrum Two apparatus with mercury cadmium telluride detector, which allowed high sensitivity measurements in the mid-infrared region. Microparticles were placed on a KBr matrix, which was used as a slide. The measuring parameters for the micro-transmission mode were spot 50 μm , 64 scans, resolution 8 cm^{-1} , spectral range 4000–550 cm^{-1} . The microparticles identified by μFTIR were larger than 10 μm . It has to be considered that 10 μm (at 1000 cm^{-1}) is the diffraction limit of IR spectroscopy, beyond which it is very difficult to obtain clear spectra (Primpke et al., 2017). The spectra were compared with a built-in database or with reference spectra specifically created for this study. A 65% matching was considered enough for positive identification according to the previous studies (Liu et al.,

2019b). In specific cases, particularly for distinguishing between polyamides and wool/silk, a case-by-case study was undertaken.

Microparticles were classified in four classes based on their chemical nature: MPs, natural (natural fragments and natural fibres, such as cellulose, wool, cotton and linen with natural colours typical of each polymer such as white or grey), artificial (fibres of extruded cellulose, or natural fibres with non-natural colours or with evidence of anthropogenic processing), and unclassified (microparticles were labelled as unclassified due to their low matching with standard spectra < 65%). The concentration of each microparticle class in the atmosphere was calculated based on the proportion of microparticles identified in the subsample and the total flow through the steel meshes as determined from air flowmeters.

2.4. Prevention of procedural contamination

To avoid sample contamination several measures were taken. All metal, steel and glass material were carefully cleaned with Milli-Q water, wrapped with aluminium foil and heated to 300 °C for 4 hours. This procedure removed all possible rests of possibly interfering fibres and other organic substances from glassware and steel filters. The use of any plastic material was avoided. To account for possible contamination during sample collection, procedural blanks (25 µm steel meshes exposed to same experimental conditions except air filtration during the flights) and control blanks (Petri dishes with 25 µm steel meshes, which were kept open during sampling inside the aircraft to identify possible contamination from indoor air) were carried out. Possible contamination during quantification and identification of the samples was assessed by procedural blanks (opening Petri dishes with 25 µm steel meshes) to evaluate the possible contamination from the surrounding environment. All procedural blanks and controls were used during quantification and identification. Microparticles similar in chemical composition to those found in samples were subtracted from the total counting. Clothing was controlled throughout the whole process. During laboratory manipulation, the clothing of people manipulating samples was controlled by using non-typical bright colours like yellow, orange or purple, 100% cotton in all cases and with the provision that such colours would be excluded from the total counting

if found. Further details are provided elsewhere (González-Pleiter et al., 2020a).

2.5. Model for atmospheric transport and deposition of microplastics

Atmospheric transport and deposition simulations were performed considering an initial unitary release at the median altitude of flight above Madrid. The simulations were performed using the HYbrid Single-Particle Lagrangian Integrated Trajectory (HYSPLIT) model (Draxler and Rolph, 2010; Stein et al., 2015), developed by the National Oceanic and Atmospheric Administration (NOAA) Air Resources Laboratory (Rolph et al., 2017). This model is widely used by the atmospheric sciences community for determining atmospheric transport and dispersion of pollutants including MPs (Allen et al., 2019; Aneja et al., 2006; Kallos et al., 2007; Reche et al., 2018). The Global Data Assimilation System (GDAS) meteorological data were used to feed HYSPLIT model mimicking the samples acquired during the flight. For simulations, the equivalent diameter of MPs (fibres and fragments) found above Madrid were calculated and deposition was parameterized (further details in Table S2 and supplementary section 1, SM).

3. Results

3.1. Occurrence and characterization of microparticles

A total set of 323 microparticles was found in the samples taken during the flights over high-density urban, low-density urban, sub-rural and rural areas of Central Spain (Table S1, SM). According to shape, microparticles were primarily classified into fragments and fibres. For the sake of clarity, a classification of the terms used in this work is given in Fig. S1 (SM). The dominant shape of microparticles found above sub-rural and rural areas were fibres, which represented up to 84 % of the microparticles, while in flights over urban areas, fragments represented up to 67 % of the microparticles. Equivalent diameters were calculated from recorded micrographs. For fragments, projected area diameter was used, while for fibres the equivalent diameter was defined as the aerodynamic diameter as calculated from the Harris-Fraser equation that describes fibre volume in terms of prolate spheroids (Gonda and Abd El Khalik, 1985) (see details in Table S2, SM). The majority of

collected microparticles (59.6 %) had equivalent diameters in the 10-70 μm range (Fig. 2). Some microparticles with equivalent diameter smaller than mesh opening size (25 μm) were collected, most probably because of their aspect ratio and orientation. Fibres ranged from 84-1709 μm length (average 662 μm , median 675 μm) and 4-97 μm width (average 25.4 μm , median 20 μm). Fragments ranged from 42-815 μm length (average of 204 μm , median 142 μm) and in 17-408 μm width (average 103 μm , median 72 μm). Overall, the volume concentration of microparticles ranged from 65.4 microparticles m^{-3} collected above urban areas to 13.8 microparticles m^{-3} in samples taken above rural zones. The highest abundance of microparticles was observed when sampling above Central Madrid, a highly populated area (about 3.2 million inhabitants). Lower values (39.4 microparticles m^{-3}) were observed in the atmosphere above Guadalajara (city with about 86 000 inhabitants) and the lowest in flights above sub-urban and rural areas. Fig. 2 breaks up microparticles in terms of class as explained below. The category corresponding to smaller sizes (< 30 μm) was not the most populated one because it included particles or fibres that depending on their orientation can be retained or not.

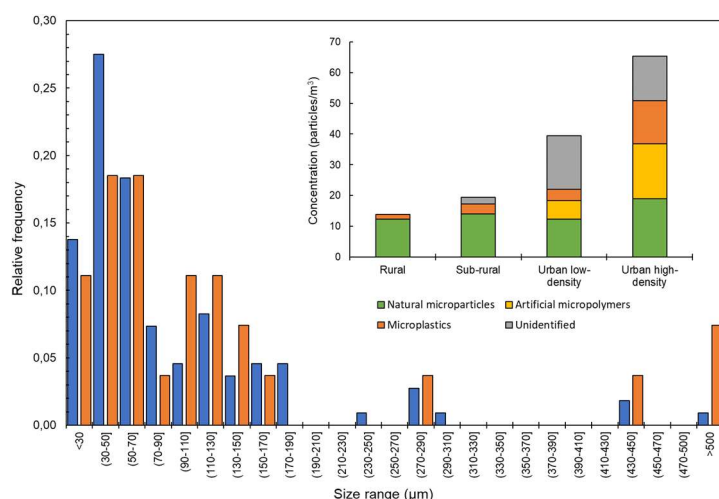


Figure 2. Size distribution based on equivalent diameter for the three flights. Blue bars for all microparticles, orange for MPs. Inset: volume concentration for the different class of microparticles: natural microparticles, artificial microparticles, MPs and unidentified microparticles.

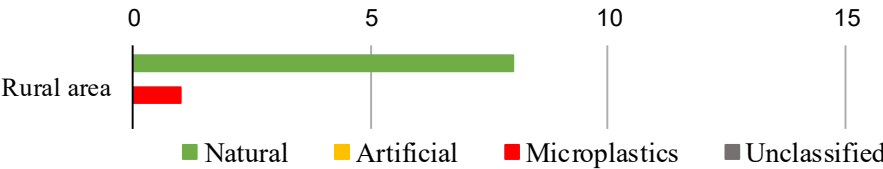
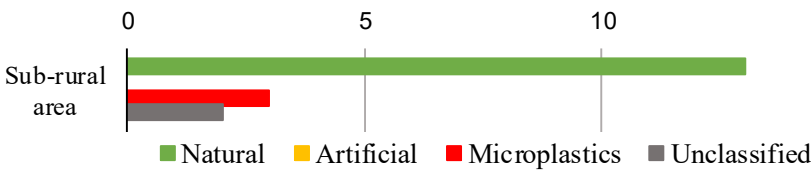
A subsample of 113 microparticles, one third of the total amount retained in the filters was analysed by μFTIR to elucidate their chemical composition (see additional details in Table S1, SM). The results of the analyses allowed discriminating

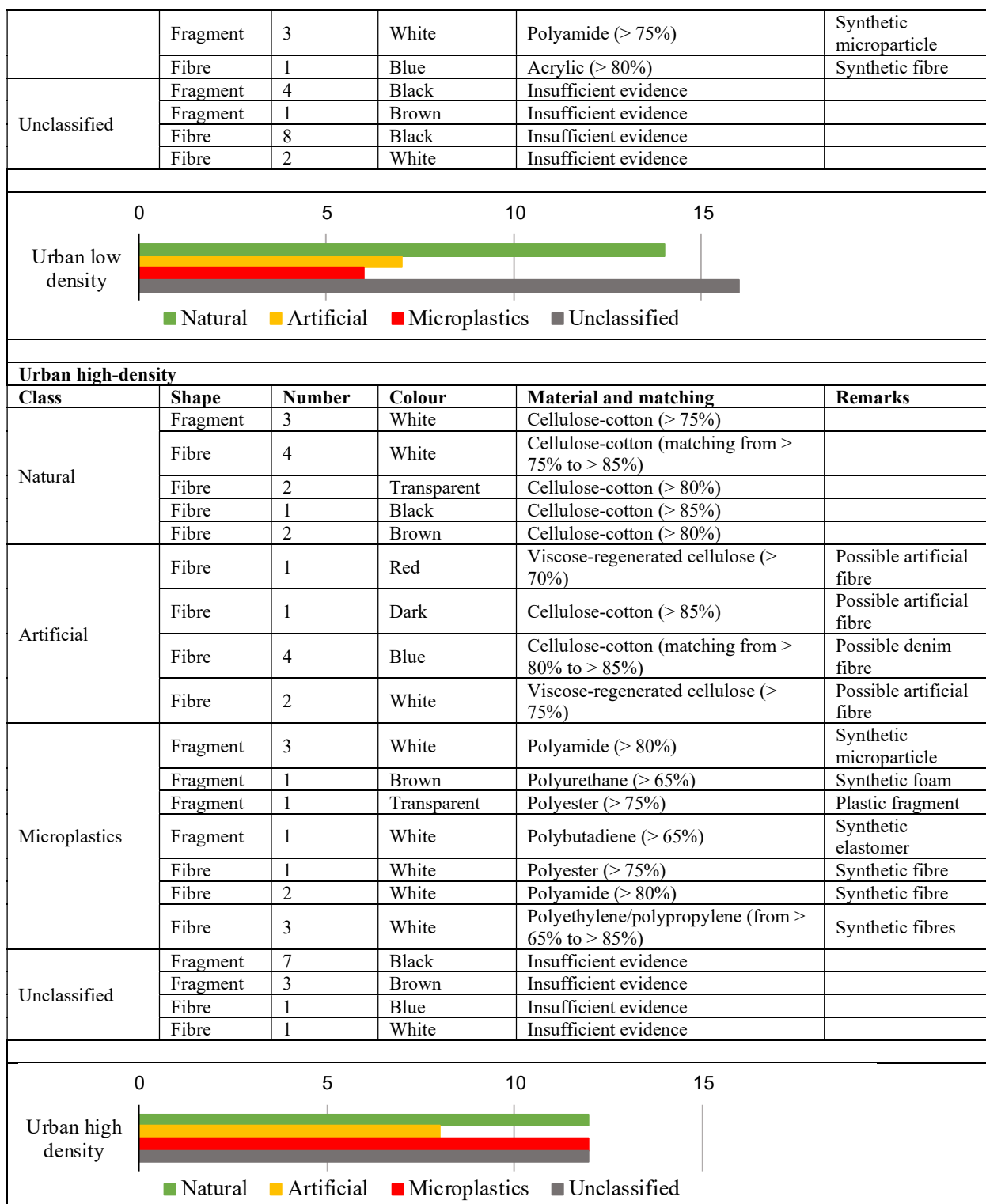
among natural microparticles (mostly cellulose or wool), artificial materials (which are all fibres and therefore defined in ISO/TR 11827 Textiles — Composition testing — Identification of fibres) and MPs (synthetic polymers). Size distribution of MPs and the concentration of all classes of microparticles in the four tested locations are shown in Fig. 2. The full set of results is summarized in Table 1.

The identification of sampled microparticles showed the presence of MPs, natural and artificial microparticles as well as a residual class of unclassified microparticles in different proportions. Natural microparticles predominated over rural areas, while MPs were present in all samples and were abundant in urban areas. The proportion of natural microparticles was higher above rural (89.1 %) and sub-rural samples (72.3 %) rather than in those taken over urban areas (31.4 % and 29.0 %). The concentration of MPs ranged from 13.9 MPs m^{-3} (Madrid) to 1.5 MPs m^{-3} (rural areas) as shown in the inset of Fig. 2. Seven different MPs types were identified in the samples (Table 1). The highest diversity was found in flights above Madrid, while the majority of MPs identified over rural and sub-urban areas were polyester, polyamide and acrylic fibres, which accounted for > 60 % of the identified MPs. Polyurethane, polystyrene, polybutadiene and polyolefins were also found in flights above the urban areas of Guadalajara and Madrid. Artificial microparticles included fibres from extruded textiles like rayon and were only found in urban areas. Besides regenerated cellulose, natural fibres with non-natural colour were also classified as artificial fibres because of the evidence of industrial processing. The rationale is that natural fibres undergoing industrial processes are not environmentally neutral as they contain additive like dyes, flame retardants or light stabilizers, among others (O'Brien et al., 2015). Fig. 3 shows the FTIR spectra of four microparticles, three MPs and one artificial fibre together with their respective standards.

The matching between FTIR spectra and standards was > 65 % for all synthetic and artificial polymers, higher than the minimum percentage of 60 % recommended elsewhere (Liu et al., 2019a). Special care was taken for assigning fibres to polyamide. It is not always easy to distinguish between synthetic polyamide and natural silk or

Table 1. Microparticle classes found in samples. The graphs inside show the absolute frequency by class.

Rural area					
Class	Shape	Number	Colour	Material and matching	Remarks
Natural	Fragment	5	White	Cellulose (matching 50-60%)	
	Fibre	3	White	Cellulose-cotton (> 75%)	
Artificial	-				
Microplastics	Fibre	1	White	Polyester (> 85%)	Synthetic fibre
Unclassified	-				
 <p>0 5 10 15</p> <p>Rural area</p> <p>■ Natural ■ Artificial ■ Microplastics ■ Unclassified</p>					
Sub-rural area					
Class	Shape	Number	Colour	Material and matching	Remarks
Natural	Fragment	1	White	Wool (> 85%)	
	Fragment	1	Black	Wool (> 80%)	
	Fragment	1	Green	Cellulose-cotton (> 65%)	
	Fibre	4	Translucid	Cellulose-cotton (matching > 65%)	
	Fibre	4	White	Cellulose-cotton (matching from > 65% to > 80%)	
	Fibre	1	White	Wool (> 60%)	
	Fibre	1	Black	Cotton (> 90%)	
Artificial	-				
Microplastics	Fibre	1	Red	Polyester (> 60%)	Synthetic fibre
	Fibre	1	White	Acrylic (> 75%)	Synthetic fibre
	Fibre	1	Green	Polyamide (>75%)	Synthetic fibre
Unclassified	Fragment	2	Black	Insufficient evidence	
 <p>0 5 10 15</p> <p>Sub-rural area</p> <p>■ Natural ■ Artificial ■ Microplastics ■ Unclassified</p>					
Urban low-density					
Class	Shape	Number	Colour	Material and matching	Remarks
Natural	Fragment	2	White	Cellulose-cotton (> 80%)	
	Fragment	2	White	Wool (> 70%)	
	Fibre	4	White	Cellulose-cotton (matching from > 65% to > 85%)	
	Fibre	1	Black	Cellulose-cotton (> 85%)	
	Fibre	1	Black	Wool (> 65%)	
	Fibre	1	White	Wool (> 65%)	
	Fibre	1	Transparent	Cellulose-cotton (> 75%)	
	Fibre	1	White-reddish	Cellulose-cotton (> 85%)	
	Fibre	1	Brown	Cellulose-cotton (> 70%)	
Artificial	Fibre	3	Blue	Cellulose-cotton (> 80%)	Possible denim fibre
	Fibre	1	Blue	Wool (> 65%)	Possible anthropogenic fibre
	Fibre	1	White-reddish	Wool (> 65%)	Possible anthropogenic fibre
	Fibre	1	Dark	Viscose-regenerated cellulose (> 65%)	Possible artificial fibre
	Fibre	1	Brown	Cellophane-regenerated cellulose (> 80%)	Possible artificial fibre
Microplastics	Fragment	1	Black	Polyurethane (>75% polyether urethane)	Elastomer
	Fragment	1	Grey	Polystyrene (> 95%)	Possible packaging material



wool because FTIR spectra look similar and the shift of absorbance maxima are usually too small. The main difference is the width of the band at 3000-3500 cm⁻¹, due to the stretching vibration of N-H and O-H (adsorbed water), which is broader for natural products. Besides C=O stretching and C-N-H bending bands at ~1640 cm⁻¹ and ~1530 cm⁻¹, respectively are sharper in synthetic materials. Generally, these differences are enough for discriminating between natural and synthetic materials, when working in reflectance mode, but

results are less concluding when analysing thin or degraded fibres from environmental samples in transmission mode (Peets et al., 2019). In this work, we attributed to natural materials (wool) spectra with matching < 75 % with synthetic polyamide standards and with the presence of strong bands in the 3000-3500 cm⁻¹ region. Conversely, matching > 75 % and spectra without broad N-H stretching bands were considered evidence of synthetic polyamide. Fig. S3 (SM) shows spectra of two white fibres identified one

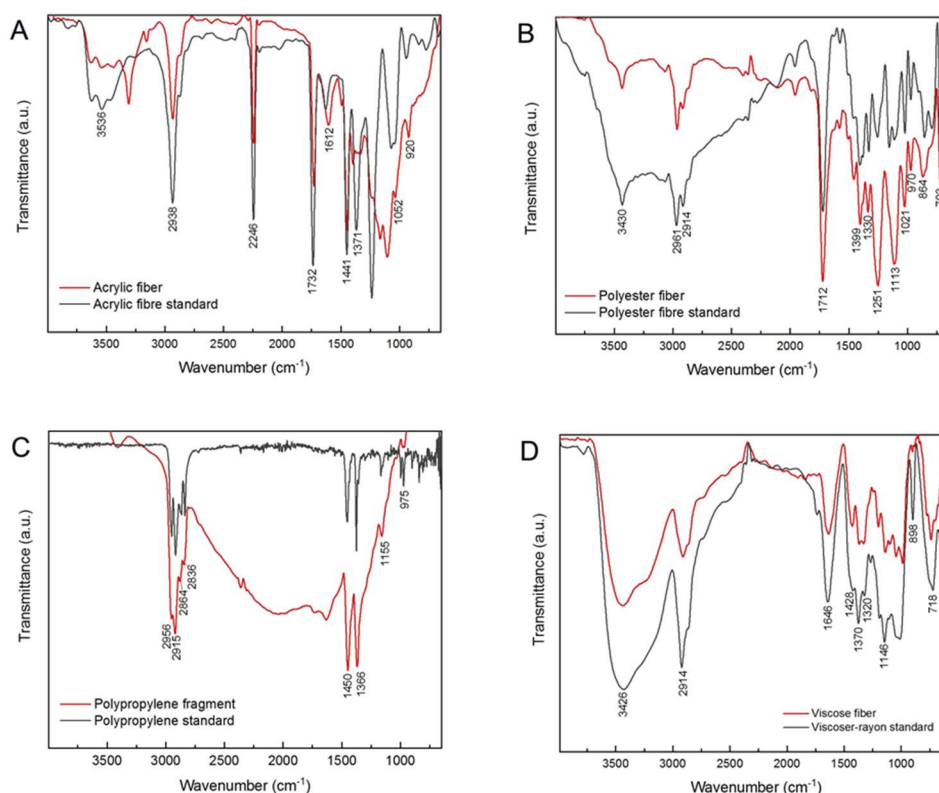


Figure 3. μ FTIR spectra of one acrylic fibre (A), one polyester fibre (B), one polypropylene fragment (C) and one viscose fibre (D) accompanied by their corresponding standard.

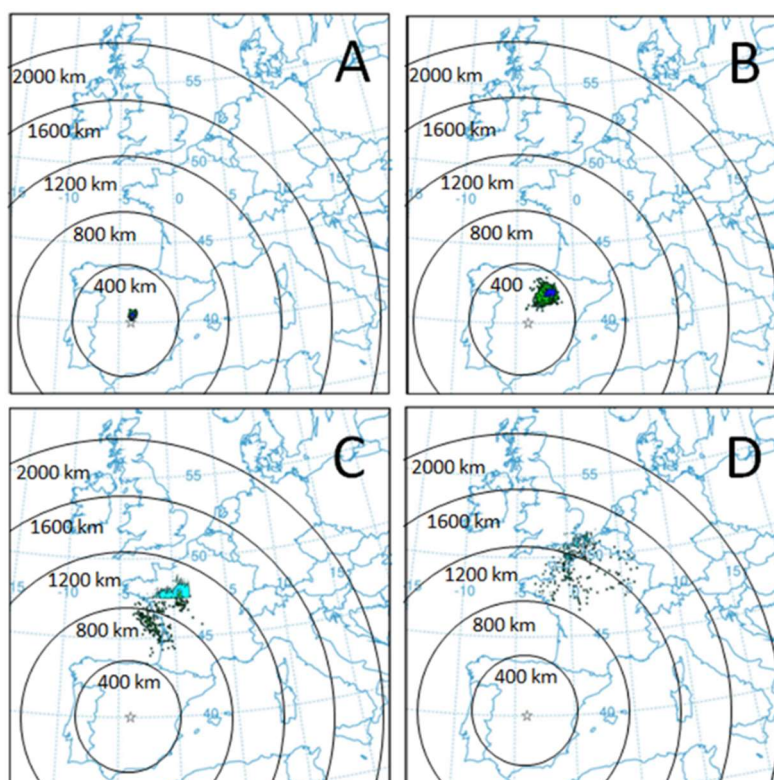


Figure 4. Simulation of deposition pattern of MPs collected during the flight above the high-density area of Madrid using NOAA HYSPLIT model. The results correspond to a representative size of sampled MPs. Simulations were performed for 1 h (A), 12 h (B), 24 h (C) and 36 h (D) with an initial mass release calculated based on MPs concentration measured in the sampling area at the altitude, day, and time of sampling and assuming that MPs were homogeneously distributed in the sampled region of Central Madrid (further details in Table S2, Supplementary Materials). The colours represent the order of magnitude of deposition values (yellow: $> 1.0 \times 10^2$ MPs m^{-2} ; blue 1.0×10^1 MPs m^{-2} ; green: 1.0×10^0 MPs m^{-2} ; turquoise: $> 1.0 \times 10^{-1}$ MPs m^{-2}).

as wool (not silk because of the absence of the characteristic silk band $\sim 1710\text{ cm}^{-1}$) and the other as synthetic polyamide.

3.2 Atmospheric transport and deposition of microplastics

Fig. 4 shows the deposition pattern for the representative MPs found for the flight above Madrid, a high-density urban area. The simulations performed for Madrid indicated that MPs were transported $\sim 400\text{ km}$ reaching the north of Spain after 24 hours (Fig. 4B). A significant fraction of the simulated MPs was dispersed far away from their source location reaching Central Europe and, eventually, the south of United Kingdom, France and Belgium, more than one thousand kilometres away from their point of sampling, supposedly close to their source (Fig. 4C and 4D). According to the simulations, a fraction of MPs remained in the atmosphere after 36 h (Table S3, SM), allowing them to reach very distant places. Likewise, this implies that the MPs collected in our flights cannot be strictly allocated in origin. In this sense, considering the south-southeasterly winds recorded during the flight above urban areas, it is probable that the Guadalajara sample was influenced by emissions from Madrid urban area.

4. Discussion

Our results showed that the concentration of microparticles tended to decrease when moving away from urban areas (Fig. 2). This result agreed with previous studies performed at ground level in different places (Liu et al., 2019b). Interestingly, the shape, size and chemical composition of microparticles also changed depending on the sampling area. Concerning shape, literature studies differ. Fragments were the dominant shape of microparticles recovered from urban areas and were in average larger than those collected over rural and sub-rural areas. On the contrary, fibres were the dominant shape in rural and sub-rural samples. The most probable explanation is that the origin of a significant fraction of the collected particles is in the highly populated area of Madrid. It is important to note that the flight above Madrid overflowed the centre of the city over its main avenue. The literature results on the shape of particles found in the atmospheric fallout is controversial. Some studies carried out in or in the neighbourhood of

populated cities showed that the MPs were mainly fibres (Cai et al., 2017; Dris et al., 2015). However, a study reporting the concentration of MPs in the atmospheric deposition from the metropolitan region of Hamburg showed fragments dominating as compared to fibres (Klein and Fischer, 2019). The differences can be attributed to local emission sources such as highways, the presence of forests or different meteorological conditions. It is important to consider that all data available to date correspond to atmospheric precipitation and not to direct observations in the atmosphere. Overall, the results suggested that densely populated cities are an important source of microparticles and may significantly contribute to the pollution due to anthropogenic substances in the atmospheric compartment. In fact, compared to air sampled in Shanghai, a higher concentration of microparticles was observed in Madrid, probably due to the higher population density of Madrid: Shanghai: $2059\text{ inhabitants/km}^2$, Madrid: $5266\text{ inhabitants/km}^2$ (Liu et al., 2019a). Higher surface temperature might cause microparticles emitted near ground level to rise from surface and to reach high altitude in the atmosphere, eventually going beyond the PBL (Klein and Fischer, 2019; Liu et al., 2019a).

The simulations performed allowed calculating the rate of deposition of MPs. This calculation can be performed based on the total number of MPs estimated for the sampled area of Central Madrid (84 km^2 as shown in Fig. S4, SM), the sampled height (1500-2500 m a.g.l.) and the average MPs concentration (13.9 MPs m^{-3} ; see details in the Table S1, SM). Using the median size of MPs, assuming homogeneous distribution within the sampled region, and multiplying the total concentration of MPs by the sampled area above the Central Madrid, the number of MPs could be roughly estimated as 11.6×10^{11} MPs between 1500 and 2500 m a.g.l. (see details in Table S2, SM). Predicted deposition values yielded cumulative deposition in the $100\text{--}117\text{ MPs m}^{-2}$ range for the first 24 hours, which corresponded to the yellowish spots of Fig. 4. One tenth of these values corresponded to blue spots and one hundredth to green coloured spots. The simulation resulted in expected deposition rates in the $0.1\text{--}10\text{ MP m}^{-2}\text{ day}^{-1}$ range for the Bay of Biscay solely attributed to the MPs sampled over Madrid 24 h before (Fig. 4C). A comparison with literature data obtained from ground-level

samplings can be performed. A selection of relevant results of deposition rates observed at ground level is given in Table 2. The literature data point towards deposition rates for MPs in the order of the hundreds of MPs per square meter and day without clear difference between urban, rural and even remote areas. It should be noted that all previous deposition studies measured MPs deposited or collected near the ground, whereas this work evaluated the fate of MPs directly

sampled at high altitude at a given place and time. We analysed the trajectory of MPs and predicted their deposition rate in the first approach to this kind reported up to date. It is important to note that ground and altitude sampling represent two different and complementary approaches, the latter opening a new area in a field with very limited data. In fact, the data reported here are the first direct sampling of MPs in the atmosphere.

Table 2. Literature data for the deposition rate of microparticles/microplastics.

Place	Shape	Size (µm)	Polymer type	Deposition rate	Reference
Paris, urban	Mostly (90%) fibres	100-5000	No chemical identification performed	29-280 (average: 118)*	Dris et al., 2015
Paris, urban	Mostly fibres	50-5000	Natural fibres (50%), synthetic fibres (12%), synthetic polymers (17%)	2 -350 (average: 110 ± 96 and 53 ± 38; two sites)*	Dris et al. 2016
China, urban	All forms	< 200-4200	Synthetic polymers	(average: 31 ± 8 – 43 ± 4)**	Cai et al., 2017
Pyrenees, remote area	All forms	< 25-3000 (<50-600 square root of projected area)	Synthetic polymers	(average: 365 ± 69)*	Allen et al., 2019
Hamburg, urban & periurban	Mostly fragments	< 63-5000	Synthetic polymers (77%)	136.5-512.0**	Klein and Fisher, 2019

* Microparticles m⁻² day⁻¹

** MPs m⁻² day⁻¹

Based on our findings, MPs can be transported and dispersed hundreds and even thousands of km from their initial release location until they are finally deposited. These results can help explain how MPs may reach remote areas where there are not significant anthropogenic activities in the vicinity (Allen et al., 2019; Ambrosini et al., 2019; Free et al., 2014; Zhang et al., 2016; Zhang et al., 2019). So far, very few studies have focused on the atmospheric transport of MPs. Strictly speaking, ground-level sampling does not allow to unambiguously determine their origin. However, their most probable source are densely populated areas. In this work, we demonstrated that atmospheric transport may play a significant role in the long-range transport of small MPs, supporting the hypothesis that MPs can move between distant areas and countries in a few days, at least for MPs with size not larger than the tens of microns. Due to their low concentration in the atmosphere, and the difficulty to filtrate a high volume of air during flight time, the number of particles collected in this work was not high. However, this is the first time MPs are directly collected from the atmosphere at high altitude, thereby proving their presence even above the

PBL. Further research would be needed to clarify the role of the atmosphere as a dispersion pathway of MPs by studying different areas, time periods, and altitudes, and aircraft missions would be a valuable tool for it.

4. Conclusions

In this ground-breaking study, we obtained direct evidence of the presence of MPs in the atmosphere at high altitude. We used aircrafts to collect samples above planetary boundary layer and detected higher concentration of microparticles and MPs when flying above densely populated areas. Seven types of synthetic polymers, either as fibres or as fragments, extruded textiles and industrially processed fibres were identified, and their concentration calculated. Our findings demonstrated for the first time the assumption that MPs are present in the atmosphere hundreds of meters above ground level. Atmospheric transport and deposition simulations using our results, indicated that urban areas could be sources of MPs, which may eventually end up in distant areas. This work shed light on the atmospheric long-range transport of

MPs showing how they can constitute a global pollution issue.

Acknowledgements

C212 airborne access was generously provided by INTA, coordinated by the Aerial Platform for Research team and with the logistic and operational support of Group 47 of the Spanish Air Force. The authors gratefully acknowledge the NOAA Air Resources Laboratory (ARL) for the provision of the HYSPLIT transport and dispersion model. We also acknowledge support from the EnviroPlaNet Network Thematic Network of Micro- and Nanoplastics in the Environment (RED2018-102345-T; Ministerio de Ciencia, Innovación y Universidades). We thank the financial support provided by the Spanish Ministerio de Ciencia, Innovación y Universidades (CTM2016-74927-C2-1-R/2-R, CGL2015-69758-P, CGL2017-92086-EXP, RTI2018-094867-B-I00) and National Institute for Aerospace Technology (PAI/APL/001/09).

References

- Abbasi S, Keshavarzi B, Moore F, Turner A, Kelly FJ, Dominguez AO, et al. Distribution and potential health impacts of microplastics and microrubbers in air and street dusts from Asaluyeh County, Iran. *Environ. Pollut.* 2019; 244: 153-164.
- Allen S, Allen D, Phoenix VR, Le Roux G, Durántez Jiménez P, Simonneau A, et al. Atmospheric transport and deposition of microplastics in a remote mountain catchment. *Nat. Geosci.* 2019; 12: 339-344.
- Ambrosini R, Azzoni RS, Pittino F, Diolaiuti G, Franzetti A, Parolini M. First evidence of microplastic contamination in the supraglacial debris of an alpine glacier. *Environ. Pollut.* 2019; 253: 297-301.
- Aneja VP, Wang B, Tong DQ, Kimball H, Steger J. Characterization of major chemical components of fine particulate matter in North Carolina. *J. Air Waste Manage. Assoc.* 2006; 56: 1099-1107.
- Bergmann M, Mützel S, Primpke S, Tekman MB, Trachsel J, Gerds G. White and wonderful? Microplastics prevail in snow from the Alps to the Arctic. *Sci. Adv.* 2019; 5: eaax1157.
- Bomgardner MM. The great lint migration. *Chem. Eng. News* 2017; 95: 16-17.
- Cai L, Wang J, Peng J, Tan Z, Zhan Z, Tan X, et al. Characteristic of microplastics in the atmospheric fallout from Dongguan city, China: preliminary research and first evidence. *Environ. Sci. Pollut. Res.* 2017; 24: 24928-24935.
- Chang X, Xue Y, Li J, Zou L, Tang M. Potential health impact of environmental micro- and nanoplastics pollution. *J. Appl. Toxicol.* 2020; 40: 4-15.
- Chen G, Feng Q, Wang J. Mini-review of microplastics in the atmosphere and their risks to humans. *Sci. Total Environ.* 2019: 135504.
- Draxler R, Rolph G. HYSPLIT (HYbrid Single-Particle Lagrangian Integrated Trajectory) model access via NOAA ARL READY website (<http://ready.arl.noaa.gov/HYSPLIT.php>). NOAA Air Resources Laboratory. Silver Spring, MD 2010; 25.
- Dris R, Gasperi J, Mirande C, Mandin C, Guerrouache M, Langlois V, et al. A first overview of textile fibers, including microplastics, in indoor and outdoor environments. *Environ. Pollut.* 2017; 221: 453-458.
- Dris R, Gasperi J, Rocher V, Saad M, Renault N, Tassin B. Microplastic contamination in an urban area: a case study in Greater Paris. *Environ. Chem.* 2015; 12: 592.
- Dris R, Gasperi J, Saad M, Mirande C, Tassin B. Synthetic fibers in atmospheric fallout: A source of microplastics in the environment? *Mar. Pollut. Bull.* 2016; 104: 290-3.
- Enyoh CE, Verla AW, Verla EN, Ibe FC, Amaobi CE. Airborne microplastics: a review study on method for analysis, occurrence, movement and risks. *Environ. Monit. Assess.* 2019; 191: 668.
- Fred-Ahmadu OH, Bhagwat G, Oluyoye I, Benson NU, Ayejuyo OO, Palanisami T. Interaction of chemical contaminants with microplastics: Principles and perspectives. *Sci. Total Environ.* 2020; 706: 135978.
- Free CM, Jensen OP, Mason SA, Eriksen M, Williamson NJ, Boldgiv B. High-levels of microplastic pollution in a large, remote, mountain lake. *Mar. Pollut. Bull.* 2014; 85: 156-163.
- Frias JPGL, Nash R. Microplastics: Finding a consensus on the definition. *Mar. Pollut. Bull.* 2019; 138: 145-147.
- Ganguly M, Ariya PA. Ice Nucleation of Model Nanoplastics and Microplastics: A Novel Synthetic Protocol and the Influence of Particle Capping at Diverse Atmospheric Environments. *ACS Earth Space Chem.* 2019; 3: 1729-1739.
- Gasperi J, Wright SL, Dris R, Collard F, Mandin C, Guerrouache M, et al. Microplastics in air: Are we breathing it in? *Curr. Opin. Environ. Sci. Health* 2018; 1: 1-5.
- GESAMP. Guidelines for the monitoring and assessment of plastic litter in the ocean. In: Kershaw PJ, Turra A, Galgani F, editors. Rep. Stud. GESAMP No. 99. IMO/FAO/UNESCO-IOC/UNIDO/WMO/IAEA/UN/UNEP/UNDP/IS A Joint Group of Experts on the Scientific

- Aspects of Marine Environmental Protection, 2019, pp. 130.
- Gonda I, Abd El Khalik AF. On the calculation of aerodynamic diameters of fibers. *Aerosol Sci. Technol.* 1985; 4: 233-238.
- González-Pleiter M, Edo C, Casero-Chamorro MC, Aguilera Á, González-Toril E, Wierzbos J, et al. Viable Microorganisms on Fibers Collected within and beyond the Planetary Boundary Layer. *Environ. Sci. & Technol. Letters* 2020a; DOI: 10.1021/acs.estlett.0c00667.
- González-Pleiter M, Velázquez D, Edo C, Carretero O, Gago J, Barón-Sola A, et al. Fibers spreading worldwide: Microplastics and other anthropogenic litter in an Arctic freshwater lake. *Sci. Total Environ.* 2020b; 722: 137904.
- Kallos G, Astitha M, Katsafados P, Spyrou C. Long-range transport of anthropogenically and naturally produced particulate matter in the Mediterranean and North Atlantic: Current state of knowledge. *J Appl. Meteorol. Clim.* 2007; 46: 1230-1251.
- Karbalaei S, Hanachi P, Walker TR, Cole M. Occurrence, sources, human health impacts and mitigation of microplastic pollution. *Environ. Sci. Pollut. Res.* 2018; 25: 36046-36063.
- Kaya AT, Yurtsever M, Bayraktar SÇ. Ubiquitous exposure to microfiber pollution in the air. *Eur. Phys. J. Plus* 2018; 133: 488.
- Klein M, Fischer EK. Microplastic abundance in atmospheric deposition within the Metropolitan area of Hamburg, Germany. *Sci. Total Environ.* 2019; 685: 96-103.
- Knight LJ, Parker-Jurd FNF, Al-Sid-Cheikh M, Thompson RC. Tyre wear particles: an abundant yet widely unreported microplastic? *Environ. Sci. Pollut. Res.* 2020.
- Kole PJ, Löhr AJ, Van Belleghem FG AJ, Ragas AMJ. Wear and Tear of Tyres: A Stealthy Source of Microplastics in the Environment. *Int. J. Environ. Res. Public Health* 2017; 14: 1265.
- Liu K, Wang X, Fang T, Xu P, Zhu L, Li D. Source and potential risk assessment of suspended atmospheric microplastics in Shanghai. *Sci. Total Environ.* 2019a; 675: 462-471.
- Liu K, Wang X, Wei N, Song Z, Li D. Accurate quantification and transport estimation of suspended atmospheric microplastics in megacities: Implications for human health. *Environ. Int.* 2019b; 132: 105127.
- Liu K, Wu T, Wang X, Song Z, Zong C, Wei N, et al. Consistent Transport of Terrestrial Microplastics to the Ocean through Atmosphere. *Environ. Sci. Technol.* 2019c; 53: 10612-10619.
- O'Brien JW, Thai PK, Brandsma SH, Leonards PEG, Ort C, Mueller JF. Wastewater analysis of Census day samples to investigate per capita input of organophosphorus flame retardants and plasticizers into wastewater. *Chemosphere* 2015; 138: 328-334.
- Peets P, Kaupmees K, Vahur S, Leito I. Reflectance FT-IR spectroscopy as a viable option for textile fiber identification. *Heritage Sci.* 2019; 7: 93.
- Primpke S, Lorenz C, Rascher-Friesenhausen R, Gerdt G. An automated approach for microplastics analysis using focal plane array (FPA) FTIR microscopy and image analysis. *Anal. Methods* 2017; 9: 1499-1511.
- Reche I, D'Orta G, Mladenov N, Winget DM, Suttle CA. Deposition rates of viruses and bacteria above the atmospheric boundary layer. *ISME J.* 2018; 12: 1154.
- Rolph G, Stein A, Stunder B. Real-time environmental applications and display sYstem: READY. *Environ. Model. Softw.* 2017; 95: 210-228.
- Sharma S, Chatterjee S. Microplastic pollution, a threat to marine ecosystem and human health: a short review. *Environ. Sci. Pollut. Res.* 2017; 24: 21530-21547.
- Stanton T, Johnson M, Nathanail P, MacNaughtan W, Gomes RL. Freshwater and airborne textile fibre populations are dominated by 'natural', not microplastic, fibres. *Sci. Total Environ.* 2019; 666: 377-389.
- Stein A, Draxler RR, Rolph GD, Stunder BJ, Cohen M, Ngan F. NOAA's HYSPLIT atmospheric transport and dispersion modeling system. *Bull. Am. Meteorol. Soc.* 2015; 96: 2059-2077.
- Wang L, Wu W-M, Bolan NS, Tsang DCW, Li Y, Qin M, et al. Environmental fate, toxicity and risk management strategies of nanoplastics in the environment: Current status and future perspectives. *J. Hazard. Mater.* 2021; 401: 123415.
- Wright SL, Ulke J, Font A, Chan KLA, Kelly FJ. Atmospheric microplastic deposition in an urban environment and an evaluation of transport. *Environ. Int.* 2020; 136: 105411.
- Zhang K, Su J, Xiong X, Wu X, Wu C, Liu J. Microplastic pollution of lakeshore sediments from remote lakes in Tibet plateau, China. *Environ. Pollut.* 2016; 219: 450-455.
- Zhang Y, Gao T, Kang S, Sillanpää M. Importance of atmospheric transport for microplastics deposited in remote areas. *Environ. Pollut.* 2019; 254: 112953.
- Zhou Q, Tian C, Luo Y. Various forms and deposition fluxes of microplastics identified in the coastal urban atmosphere. *Chin. Sci. Bull.* 2017; 62: 3902-3910.

SUPPLEMENTARY MATERIAL

Occurrence and long-range transport of microplastics sampled within and above the planetary boundary layer

Miguel González-Pleiter^{a,b,*,1}, Carlos Edo^{b,1}, Ángeles Aguilera^c, Daniel Viúdez-Moreiras^c, Gerardo Pulido-Reyes^{a, d}, Elena González-Toril^c, Susana Osuna^c, Graciela de Diego-Castilla^c, Francisco Leganés^a, Francisca Fernández-Piñas^a, Roberto Rosal^b

^a Departamento de Biología, Facultad de Ciencias, Universidad Autónoma de Madrid, Cantoblanco, E-28049 Madrid, Spain.

^b Departamento de Ingeniería Química, Universidad de Alcalá, Alcalá de Henares, E-28871 Madrid, Spain.

^c Centro de Astrobiología, CAB (INTA-CSIC), Torrejón de Ardoz, Spain.

^d Eawag, Swiss Federal Institute of Aquatic Science and Technology, Ueberlandstrasse 133, 8600 Dübendorf, Switzerland

* Corresponding author: mig.gonzalez@uam.es

¹ These authors contributed equally

Contents:

Figure S1. Scheme explaining the nomenclature used in this work.

Figure S2. Flight information. Trajectories, sampling points, locations and average altitudes (a.s.l.) of the flights in which air samples were collected on April 25, 2018 (Flight 1), May 23, 2019 (Flight 2) and June 17, 2019 (Flight 3).

Figure S3. μ FTIR spectra of fibres identified as wool (A) and synthetic polyamide (B) together with their corresponding standards.

Figure S4. Estimation of the area of Madrid (high-density urban area) overflown during sampling of using Google Earth. Red line indicates flight trajectory. Yellow line indicates the sampled area.

Table S1. Details on results. (Mean absolute deviation between brackets.)

Table S2. Parameters used in the simulations performed using the HYbrid Single-Particle Lagrangian Integrated Trajectory (HYSPLIT) model

Table S3. Percentage of microparticles found in flight 3 (over Madrid) that remained in the atmosphere after 12, 24 and 36 h. Three scenarios have been simulated as a function of particle size (see Materials and Methods 2.5 and Supplementary Section 1) for the flight: small MP, median MP, large MP and a representative size of sampled MPs.

Supplementary Section 1.

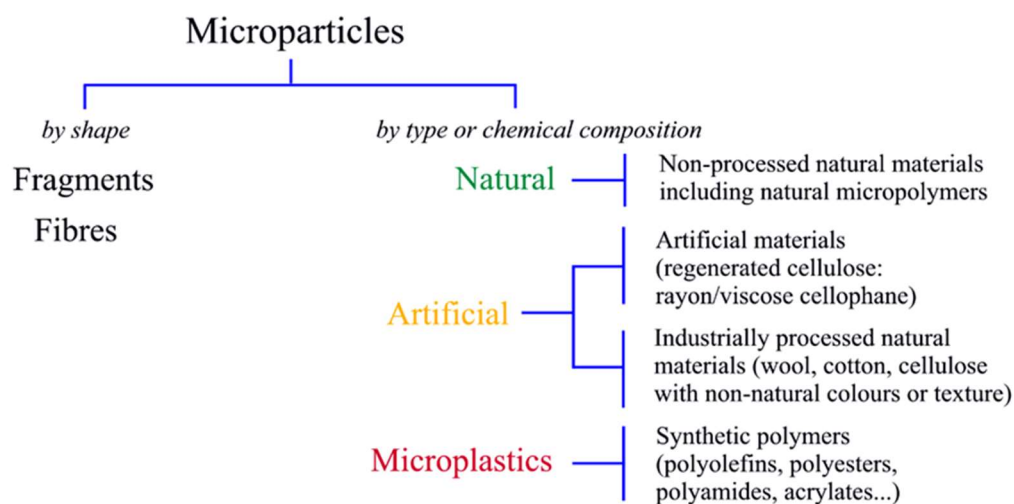


Figure S1. Scheme explaining the nomenclature used in this work.

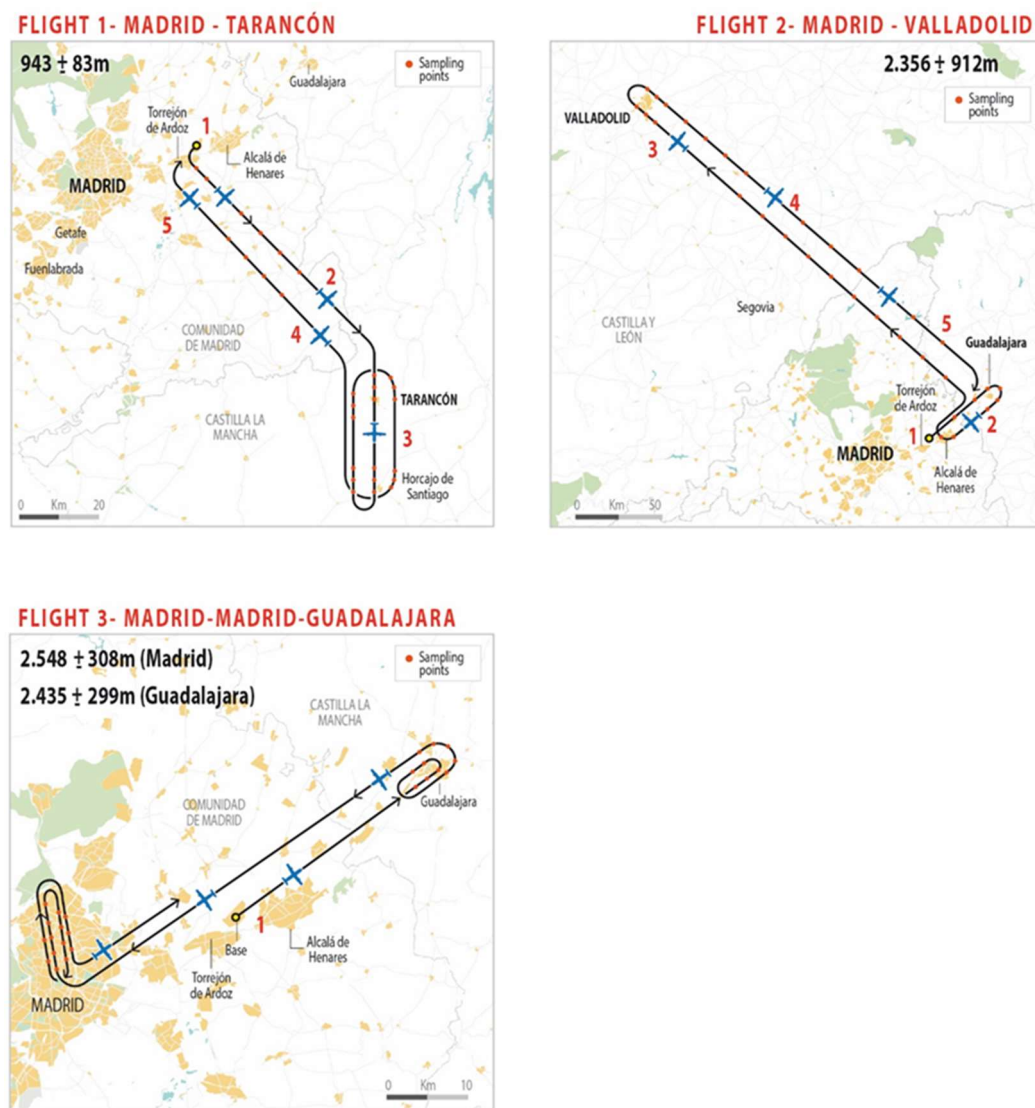


Figure S2. Flight information. Trajectories, sampling points, locations and average altitudes (a.s.l.) of the flights in which air samples were collected on April 25, 2018 (Flight 1), May 23, 2019 (Flight 2) and June 17, 2019 (Flight 3).

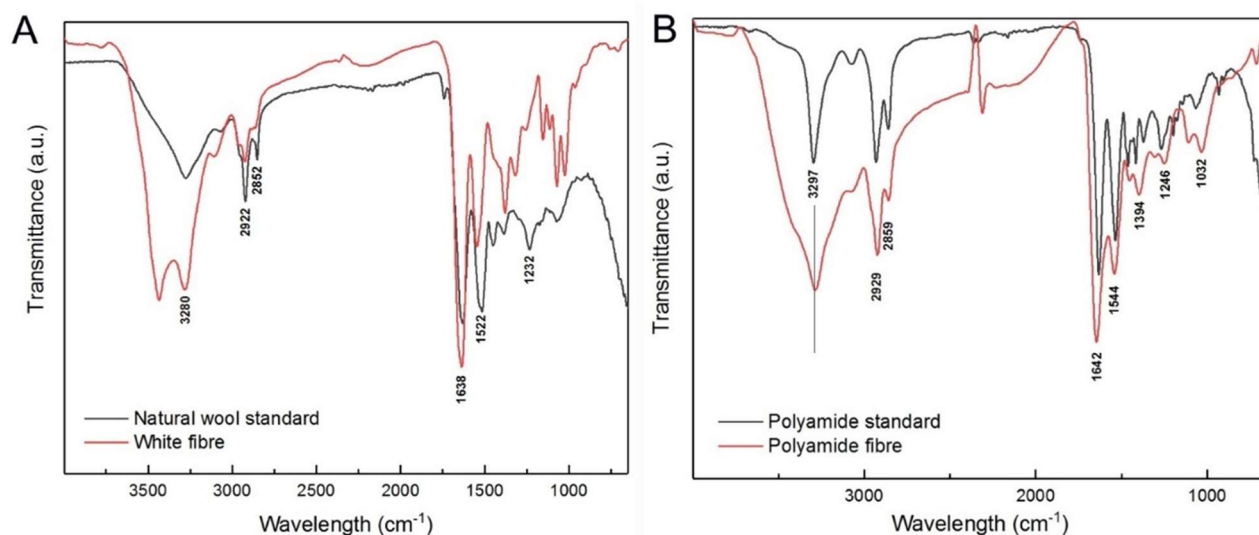


Figure S3. μ FTIR spectra of fibres identified as wool (A) and synthetic polyamide (B) together with their corresponding standards.



Figure S4. Estimation of the area of Madrid (high-density urban area) overflowed during sampling using Google Earth. Red line indicates flight trajectory. Yellow line indicates the sampled area.

Table S1. Details on results. (Mean absolute deviation between brackets.)

	Flight 1	Flight 2	Flight 3			
Area	Rural	Sub-rural	Low-density urban		High-density urban	
Samples						
Collectors location	top	top	top	side	top	side
Number of collectors	1	1	1	6	1	6
Average altitude (m) a.s.l.	943 ± 83	2356 ± 912	2435 ± 299		2549 ± 308	
Median altitude (m) a.s.l.	941	2771	2216		2800	
Total of volume of air filtered (m³)	1.30	2.52	2.48		2.68	
Volume of air filtered per filter (m³)	1.30	2.52	0.75	0.29 (0.07)	0.75	0.32 (0.08)
Total of microparticles	18	49	96		160	
Microparticles per filter	18	49	17	13.2 (6.9)	21	23.6 (6.7)
Total fibres	12	41	46		53	
Fibres per filter	12	41	8	6.2 (4.5)	8	7.4 (3.7)
Total fragments	6	8	50		107	
Fragments per filter	6	8	9	7.0 (3.6)	13	16.2 (6.3)
Average of equivalent diameter (µm)	45.7 (16.6)	67.7 (40.8)	104.2 (78.0)		85.5 (56.0)	
Median of equivalent diameter (µm)	41.2	41.3	68.3		58.0	
Microparticles analysed by µFTIR	9	18	42		44	
Microparticles analysed per filter	9	18	16	4.3 (1.6)	18	4.8 (1.0)
[Microparticles/m³]	13.8	19.5	39.4 (15.5)		65.4 (15.3)	
Natural microparticles analysed by µFTIR	8	13	14		12	
[Natural microparticles/m³]	12.3	14.1	12.4 (11.7)		19.0 (8.0)	
Artificial microparticles analysed by µFTIR	0	0	7		8	
[Artificial microparticles/m³]	0	0	5.9 (4.5)		17.9 (10.5)	
Microplastics analysed by µFTIR	1	3	6		12	
[Microplastics/m³]	1.5	3.2	3.7 (2.7)		13.9 (8.7)	
Unidentified particles after µFTIR	0	2	15		12	
[Unidentified/m³]	0	2.2	17.4 (7.8)		14.6 (8.2)	
Control + Procedural blank						
Microparticles per filter	3	6	3	2.5 (0.8)	3	2.5 (0.8)
Fibres per filter	1	3	1	1.3 (0.8)	1	1.3 (0.8)
Fragments per filter	2	3	2	1.2 (0.8)	2	1.2 (0.8)
Natural microparticles per filter	1	3	2	1.0 (0.7)	2	1.0 (0.7)
Artificial microparticles per filter	0	1	0	0	0	0
Microplastics per filter	0	0	0	0.2 (0.3)	0	0.2 (0.3)
Unidentified per filter	2	2	1	1.3 (0.8)	1	1.3 (0.8)

Table S2. Parameters used in the simulations performed using the HYbrid Single-Particle Lagrangian Integrated Trajectory (HYSPLIT) model.

HYSPLIT Dispersion model*	
Meteorological data	GDAS1
Date	17/6/2019
Time	9 (UTC +2)
Latitude	40.4167
Longitude	-3.70325
Initial released (mass) ¹	1167600000000
Release time (h) ²	1
Median altitude of sampling (m) MSL	2800
Ground level (m) MSL	665
Equivalent diameter of representative MPs (μm) found above Madrid ³	35
Concentration (mass m ⁻³) averaged between	250 ⁴ and 2800 ⁵

¹ It is an estimation assuming that MP were homogeneously distributed in the sampled region of Central Madrid. By multiplying the total concentration of microplastics by the volume of air above the sampled area of the Central Madrid, the number of MP could be roughly estimated.

[MPs] x Volume of air above Central Madrid = 1167600000000 MPs above area sampled between 1500 and 2500 meters above ground level.

[MPs] = Concentration of microplastics found above Madrid including both top and side filters 13.9 MPs/m³ (see Table S1).

Volume of air over Central Madrid = It is an estimation of the volume of air between 1500 and 2500 meters above area sampled of the Central Madrid (84 km², see details in the Figure S3) as results 84 km³

² Point release similar to sampling time

³ The aerodynamic diameters of the MPs were computed by Henn (1996)

⁴ European buildings generally do not exceed 250 meters (Pietrzak, J., 2014. Development of high-rise buildings in Europe in the 20th and 21st centuries. Challenges of Modern Technology, 5.)

⁵ Median altitude of sampling

HYPERLINK <https://www.ready.noaa.gov/HYSPLIT.php>

References

Henn, A.R. Calculation of the Stokes and Aerodynamic Equivalent Diameters of a Short Reinforcing Fiber, Part. Syst. Charact, 1996; 13: 249-253.

Table S3. Percentage of microparticles found in flight 3 (over Madrid) that remained in the atmosphere after 12, 24 and 36 h. Three scenarios have been simulated as a function of particle size (see Materials and Methods 2.5 and Supplementary Section 1) for the flight: small MP, median MP, large MP and a representative size of sampled MPs.

Flight	Simulation time	Representative MPs	Small MP size case	Median MP size case	Large MP size case
3	t = 12 h	63.7%	97.6%	27.4%	14.5%
	t = 24 h	22.9%	82.8%	1.5%	0.1%
	t = 36 h	8.1%	68.6%	0.1%	0.0%

Supplementary Section 1.

Materials and methods

Model for atmospheric deposition of microplastics. The simulations were performed for 36 h with an initial release in the sampling area (Madrid) integrated during a period < 1 h (similar to sampling time) at the day and time of sampling (17/6/2019; UTC +2). Representative MPs size was simulated for flight 3 (equivalent diameter $\sim 35 \mu\text{m}$). In addition, given the strong dependence on the deposition process by the particles size, three additional cases covering a wide range of particle sizes were considered for this flight: (i) small MP size case (equivalent diameter $\sim 10 \mu\text{m}$), (ii) median MP size case (equivalent diameter $\sim 58 \mu\text{m}$), and (iii) large MP size case (equivalent diameter $\sim 90 \mu\text{m}$). It should be noted that the most of collected MPs ($> 50\%$) had equivalent diameters in the 10-90 μm range being the majority between 10 and 50 (Fig. 2). The gross size distribution found above Madrid can be allocated within the simulated range. The fibre equivalent diameter was computed by Henn (1996) and wet deposition was parameterized by means of in-cloud and below-cloud loss rates of $8 \cdot 10^{-5} \text{ s}^{-1}$ (Rolph et al., 2017). Particle density is assumed to be 1.1 g/cm^3 . The particle deposition velocity was set to a value representative of the particle density, size and modelled altitude.

References

- Henn, A.R. Calculation of the Stokes and Aerodynamic Equivalent Diameters of a Short Reinforcing Fiber, Part. Syst. Charact, 1996; 13: 249-253.
- Rolph G, Stein A, Stunder B. Real-time environmental applications and display sYstem: READY. Environ. Model. Softw. 2017; 95: 210-228.